

# Indications for solar influence on radon signal in the subsurface of Tenerife (Canary Islands, Spain)

G. Steinitz<sup>1,a</sup>, M.C. Martin-Luis<sup>2</sup>, and O. Piatibratova<sup>1</sup>

<sup>1</sup> Geological Survey of Israel, Jerusalem, Israel

<sup>2</sup> University of La Laguna, Tenerife (Canary Islands), Spain

Received 13 February 2015 / Received in final form 23 April 2015  
Published online 10 June 2015

**Abstract.** Radon at two locations in Tenerife is investigated. The MM-0 site is located in a bunker near Teide volcano. Daily radon (DR) signals are dominated by a 12-hour (S2) periodicity. Continuous wavelet transform (CWT) analysis of day-time and night-time series results in a day-night differentiation, which does not occur in the coeval temperature and pressure. This indicates that the radon system is directly affected by rotation of Earth around its axis, and not via the pressure and/or temperature pattern. San Fernando sites are in an underground gallery, located at 2.1 and 3 km from the entrance. Alpha and gamma time series show DR signals having an S1 and a strong S2 periodicity. Sidebands occur around the S1 periodicity. The lower sideband is close to 0.9972696 cycles per day (CPD; = sidereal frequency) and the upper sideband at a symmetric frequency above. They reflect a driver containing two waveforms having periodicities of rotation of Earth around its axis and around the Sun that influences radon in a non-linear fashion, leading to the sidebands around the S1 periodicity. Observation in Tenerife of sidebands and day-night phenomena substantiates the notion that the periodic components in the diurnal and annual frequency band of radon time series are due to the influence of a component in solar radiation.

## 1 Introduction

Tenerife (Canary Islands) is the largest island (2078 km<sup>2</sup>) of the Canarian Archipelago and the world's second largest oceanic volcanic island (after Hawaii). The structure of the island is controlled by a volcano-tectonic rift system forming three axis trending N-E, N-W and N-S, with predominantly basaltic volcanism. The large Cañadas Caldera and the Teide-Pico Viejo stratovolcano are located at its center, both part of the central volcanic complex of Las Cañadas edifice, which is composed of a sequence

---

<sup>a</sup> e-mail: steinitz@gsi.gov.il

of basaltic, trachybasaltic, trachytic and phonolitic rocks [1, 2]. At least six eruptions have occurred in the last 300 years, mainly consisting of basaltic monogenetic fissure activity. The last three ones, in 1706, 1798 and 1909, occurred along the NW ridge, the most active area of the island together with El Teide-Pico Viejo Complex for the last 50 Ka [3].

The temporal variation of radon (Rn-222) in the subsurface of the island has been investigated intensively. Extensive radon mapping has been conducted at surface (soil gas) and at the deep subsurface (within galleries and wells) [4]. Monitoring of radon at shallow and deep subsurface locations showed large temporal variations, which are in part both systematically recurring at a geologic scenario and also different among them. Overviews of the variation patterns are given by [5–10]. As is the case in similar geologic scenarios primary descriptions and interpretations attribute the variation patterns to time varying subsurface gas transport due to volcanic activity combined with different degrees of above surface atmospheric influences, mainly by temperature and pressure variations. Systematic daily periodic phenomena in the radon time series as well as annual variations are considered as main indicators for the above surface atmospheric influence.

Radon variation, in general contains signals the span of which ranges from annual to daily and also to sub daily. Radon time series are composed of both periodic and non-periodic signals. The non-periodic multi-day (MD) signals have varying waveforms lasting 2 to 20–30 days. The periodic signals in the annual band are composed of annual radon (AR) signals, sometimes also a semi-annual radon signal (SAR). The daily radon (DR) signal is basically composed of a 24-hour periodicity (S1) and frequently contains higher multiples of 12-hour (S2) and also 8-hour (S3) periodicity.

The notion that the periodic signals of radon in the annual and daily frequency bands are influenced by a component in solar radiation was raised in recent years [11–17]. Analysis of long term experimental alpha and gamma measurements at laboratory conditions [11, 15, 16] as well as observations at subsurface geological environments in Israel [12–14] and in the deep underground laboratory of Gran Sasso (LNGS) in Italy [17], used several statistical indicators for identification of such influence on radon signals. This is determined, so far, by the quality of the data sets in terms of their length, continuity and relative strength of the daily signal. As described in the following, additional indications which enhance this view were found after the analysis of Radon in Tenerife, an island located at a distant geographic location from Israel and Italy.

Measurements were conducted using alpha and gamma detectors. Radon measurements were based on the detection of alpha particles utilizing Barasol probes (Algade Inc., France) with a silicon junction in a chamber located behind a diffusion barrier (filter) that eliminates the contribution of radon-220. The sensitivity of the probe is 1 cph, corresponding to an air concentration of about 50 Bq/m<sup>3</sup>. The probe has a built-in data-logger that records radon, temperature and barometric pressure. Radon measurement based on the detection of gamma rays used a gamma PM-11 detector (NaI, 2", SCA; Rotem Inc., Israel). Data were collected with a sampling period of 15-minutes, and a decimal time (UT; Day 0 = 1.1.1998) was used. Pre-processing of the time series included filling of gaps by interpolation, and removal of the long-term trend. Normalized data were used for processing in the frequency domain.

Indications for the influence of a component in solar radiation were found at two scenarios, from two locations in Tenerife (Fig. 1) site MM-0 and San Fernando (SF) gallery. A different statistical criterion was used at each scenario. One of these was the occurrence of different temporal patterns between day-time and night-time measurements. A further criterion, demonstrated below, was the occurrence of indicative sidebands alongside the primary diurnal constituents (S1, S2, S3).

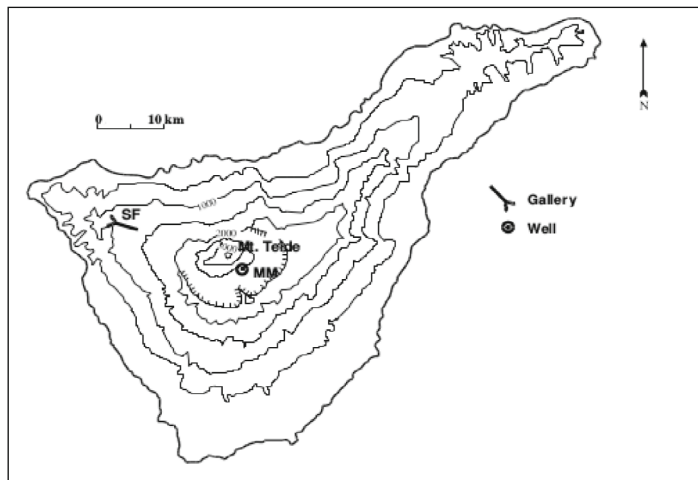


**Fig. 1.** Map of Tenerife, showing location of MM-0 (MM) and San Fernando gallery (SF). Elevation of Teide volcano 3,718 meter.

## 2 MM-0 site

MM-0 site is placed in a bunker-like concrete structure ( $4.4 \times 4.4 \times 3.9$  m), located at an elevation of 2264 m and about 600 m from the southeastern base of Teide volcano (Las Cañadas, Tenerife). The bunker is relatively isolated from the above surface air by a metal flap. This facility tops and hosts a 505 m deep borehole used by the Insular Water Council of Tenerife for hydrogeological investigation. Water level inside the well (unconfined aquifer) is at a depth of around 446 m. The lithology along the borehole corresponds to an upper layer of phonolitic and pumiceous rocks followed by basaltic lavas and some intermediate trachybasaltic flows that belong to the Teide-Pico Viejo sequence [18]. More detailed description of the lithological column of this well is given in [7]. At this site, radon and environmental variables (air temperature and barometric pressure) are recorded inside the bunker, next to the wellhead.

The radon and associated pressure and temperature measurement in the bunker span more than 1000 days, from November 15, 2007 to September 10, 2010. The temporal variation of radon in the MM-0 bunker is dominated by the daily signals with a 12-hour (S2) periodicity. Figure 2 shows two time windows demonstrating the temporal variation of the low radon level as well as the temperature in the bunker. The variation is composed of two sharp peaks per day. In some days one or both peaks may be reduced and even absent. This indicates the variation of radon in the bunker is not related to temperature. Using larger data sets this point is further elaborated below. For further analysis the measured values of radon was averaged to form a time series with a resolution of 1-hour. This time series is decomposed into two time series: a) a day-time (0800–1600 hours) time series and, b) a night-time (2000–0400 hours) time series. The gaps introduced into the time series are rectified by linear interpolation between gap ends. The same procedure was applied to the concurrent time series of pressure and temperature in the bunker. The expectation is that in the long run ( $>1000$  days) day-time and night-time measurements should yield the same patterns. Figure 3 presents the decomposed day-time and night-time time series of radon, pressure and temperature. The latter two show very similar patterns (as expected), while in the case of radon a slight dissimilarity is observable in the time domain.

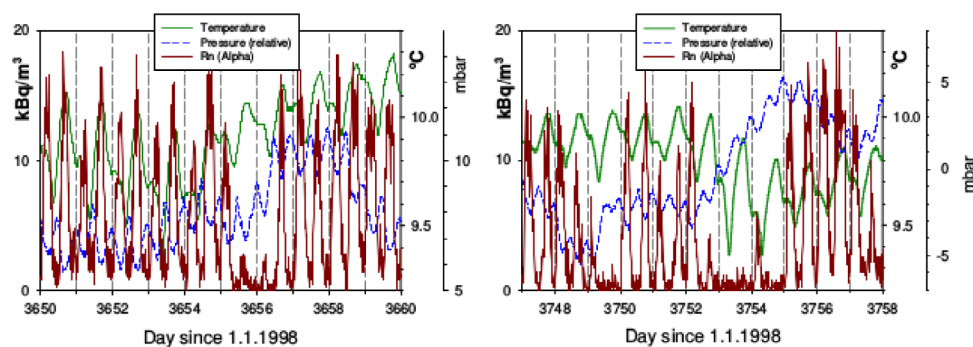


**Fig. 2.** Example 10-day long interval showing radon, atmospheric pressure and temperature variation patterns in MM-0 bunker (Day 0 = 1.1.1998). The variation of radon is dominated by two peaks per day.

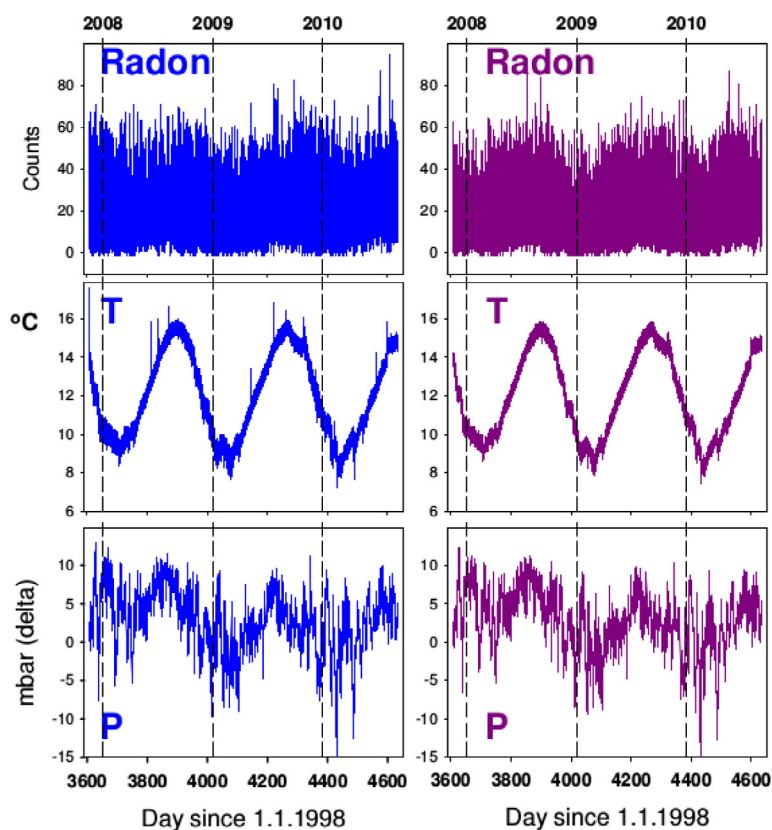


**Fig. 3.** Day-time (left column) and night-time (right column) time series of radon, temperature and pressure, at MM-0 (Day 0 = 1.1.1998).

In a further step continuous wavelet transform (CWT) analysis was performed on the day- and night-time subset time series (AutoSignal; Systat Software Inc.). The resulting patterns in the frequency-time domain are presented as Time Integrated Power Spectral Density in Fig. 4. A clear day-night differentiation is demonstrated in the case of radon. A similar day-night difference does not occur in the coeval subset time series of temperature and pressure at the site. The form and scale of the Time-Integral Squared Amplitude Power curve (black in Fig. 4) for the day- and

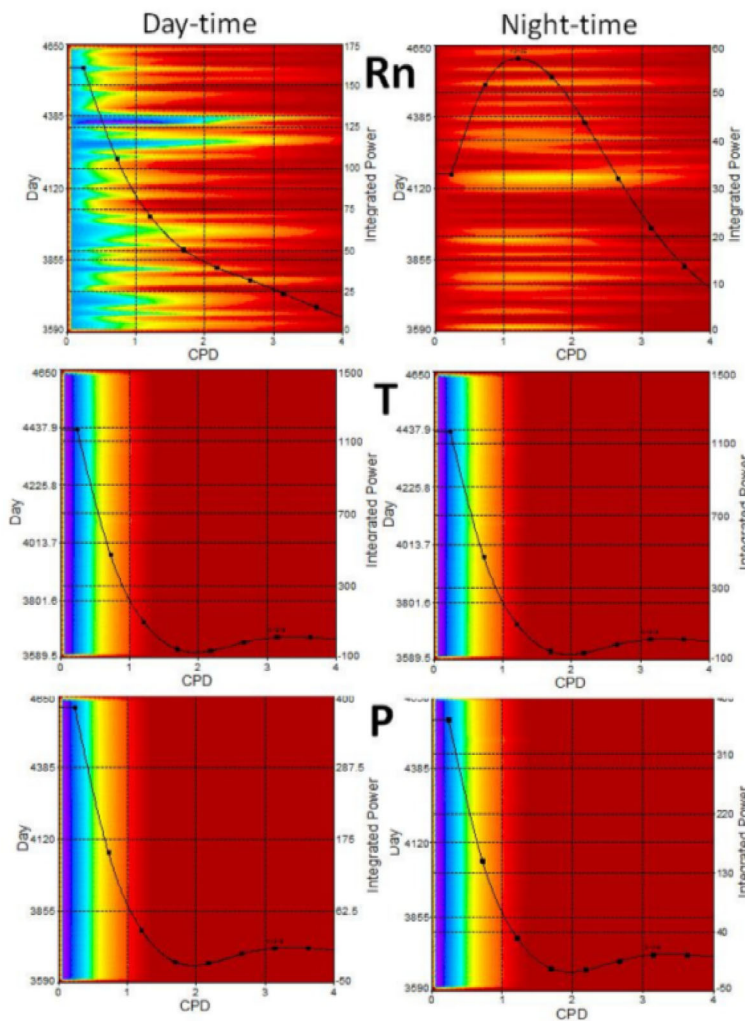


**Fig. 4.** Continuous Wavelet Transform spectral analysis of the time series shown in Fig. 3, presented as Time Integrated Power Spectral Density. The analysis is based on the Paul (complex) wavelet, with wavenumber order = 16. The curve (black) is the Time-Integral Squared Amplitude Power. Different day- and night-time patterns are obtained in the case of radon.

night-time subsets is very similar in the case of temperature and pressure, and dissimilar for radon. These differences indicate that a) neither pressure and/or temperature drive the radon system, and b) that the daily variation in radon is rather directly related to rotation of Earth around its axis, and not via temperature and/or pressure. This result, obtained in a semi-confined air volume located at near surface level, resembles a similar day-night differentiation occurring in gamma measurement of radon in a semi-confined air volume at LNGS, at a depth of 1000 m [17].

### 3 San Fernando (SF) gallery

The San Fernando gallery is a tunnel located on the NW ridge of the island (elevation 1070 m), constructed for groundwater exploitation. The tunnel is excavated in

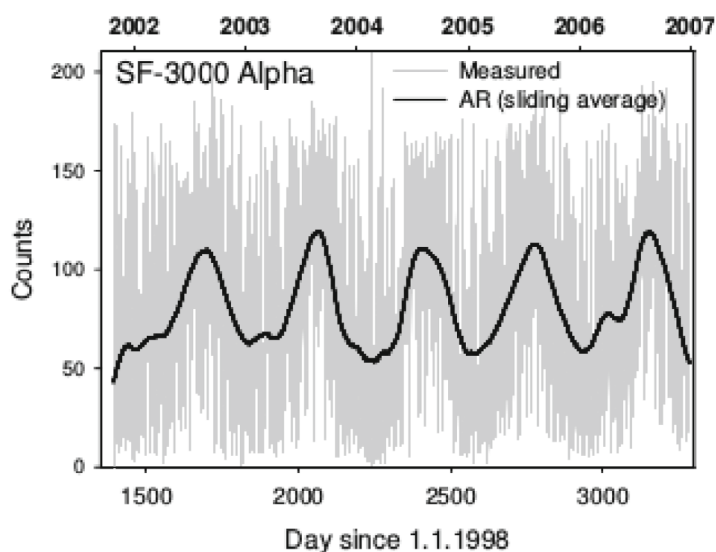


**Fig. 5.** SF-3000. Measured alpha signal and the annual radon (AR) signal applied for detrending the time series (Day 0 = 1.1.1998).

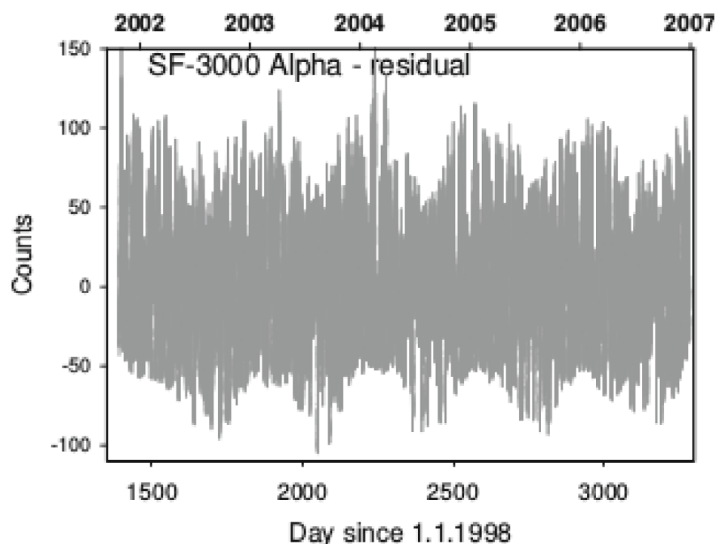


**Fig. 6.** SF-3000. The detrended (residual) alpha signal (Day 0 = 1.1.1998).

basaltic rocks and its walls are not covered. Radon monitoring is implemented at two stations located at 2142 & 3000 meter from the entrance, at depths of around 150 and 350 meters below the surface. Temperature at the sites displays long-term stability:  $19 \pm 0.3$  °C at SF-2142 (260 days) and  $16.0 \pm 0.1$  °C (300 days) at SF-3000. Alpha and gamma measurements are obtained at site SF-2142, and alpha measurements at SF-3000. Figure 5 shows the measured alpha signal at SF-3000 during an interval of around 5 years, from October 23, 2001 to December 29, 2006. The measured signal was de-trended for its long-term annual variation using a two step sliding average [5]. Using this method it is observed that the long term trend also contains a clear semiannual signal. The residual signal (Fig. 6) is dominated by a MD variation.

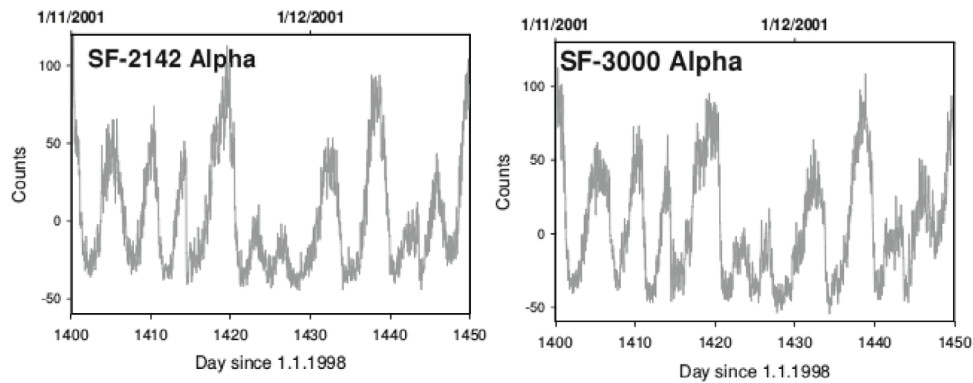


**Fig. 7.** 50-day detail of the detrended time series of alpha measurements at sites SF-2142 and SF-3000 (Day 0 = 1.1.1998). Similar level and concordant MD signal occur, exhibiting steep decreasing limbs. DR signal, of minor amplitude (10–20%) are superimposed on the MD variation.

The measured alpha and gamma time series at SF-2142 (not shown) were processed in a similar fashion. These data sets are short (gamma) and contain many data gaps. Still a clear semi-annual signal is observed in the alpha time series. The pattern of the MD signal (alpha) at the two sites is shown in Fig. 7 using the residuals for the same 50-day interval. A very high concordance of the signals is observed over the distance 850 m along the gallery. These MD signals are asymmetric with a steep decreasing flank. DR signals are superimposed on the MD signal, with amplitudes in the order of 10–20% relative to the amplitude of the MD variation.

Time series from SF sites show daily radon (DR) signals. Figure 8-left presents the spectra of the decomposed (detrended and normalized) signal in the diurnal band frequency range. At these sites the 12-hour periodicity (S2) is strong (4) relative to the fundamental diurnal S1 (24-hour) periodicity. Figure 8-right shows that sidebands (Sb) occur alongside and on both sides of the S1 frequency in the time series of all sensors. The lower sideband (LSb) occurs at a frequency close to the astronomical sidereal frequency (0.9972696 CPD). The upper sideband (USb) occurs at a symmetric frequency position relative to S1. These specific frequencies are shown as stippled vertical lines. It should be noted that: a) Sidebands at above mentioned frequencies around the S1 periodicity are manifested in the alpha and gamma measurements at site SF-2142, and in alpha measurements from SF-3000; b) the amplitude of the Sb is in the range of the amplitude of the S1 component; c) these measurements are independent; d) they are observed in spite of the relatively low count rates and in spite of the gaps in the time series, and e) in spite of the air movement at the sites. This situation is taken to indicate that these Sb reflect a genuine geophysical phenomenon.

The development of the Sb at the specific frequencies around the diurnal periodicities is attributed (P.A. Strurrock, pers. communication) to a driver containing two waveforms having periodicities of 1 day and 365.25 days, which interacts in a non-linear mode with radon in the subsurface air at the sites. The observed patterns of diurnal periodicities and associated Sb can be demonstrated using statistical simulation based on polynomial combinations of sinusoidal waveforms having these two periodicities. Thus, the observation of sidebands around S1 at the specific

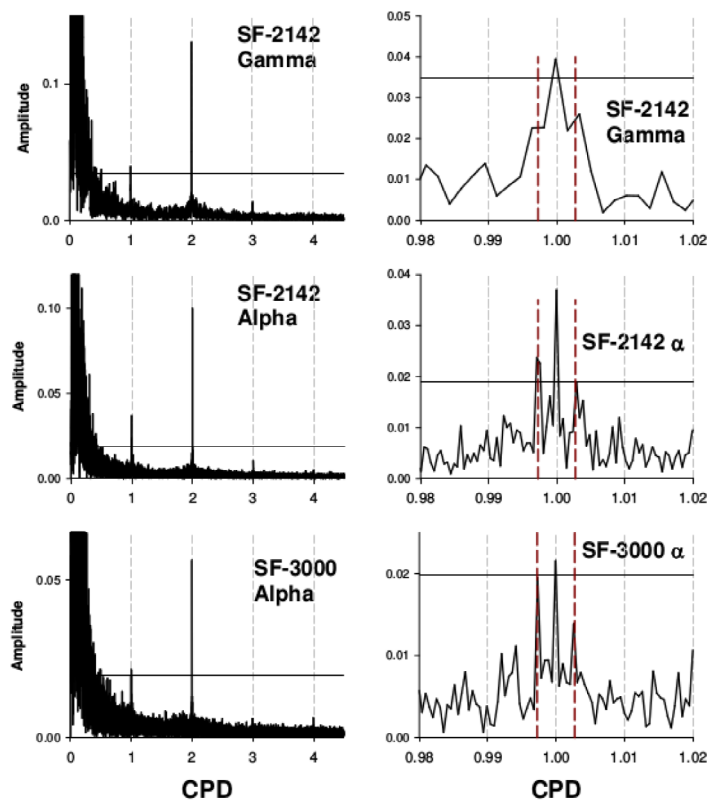


**Fig. 8.** Spectra (FFT) of de-trended time series at sites SF-2142 and SF-3000. Left column the daily variation band. Right column detail around S1 periodicity, demonstrating the occurrence of sidebands at the specific frequencies of LSb and USB (shown as vertical lines).

periodicities indicates that the periodic signals in radon time series are directly related to the cyclic rotational relations in the Earth-Sun system.

## 4 Conclusion

The observation in Tenerife of sidebands and day-night phenomena, at near surface and at depth locations, substantiates the notion that the periodic components in the diurnal and annual frequency band of radon time series are due to the influence of a component in solar radiation. This notion was first raised based on observations in Israel at sites to a depth in the order of 100 m [11–13] and later from measurements in Italy [17] at 1000 m below surface. A day-night differentiation at a subsurface location was first shown in the latter case. An important indication for such phenomena is given by [19] who show for both radon (Rn-222) and thoron (Rn-220) a day/night differentiation in the lower atmosphere. Further confirmation was obtained in the first simulation experiments using enhanced radon levels within confined volumes [15,16]. Investigation of these phenomena in radon measurements at different points on Earth has a considerable potential in two aspects: a) presenting a new frame of interpretation and new applications in the Earth sciences; b) provide important data and information related to the understanding of fundamental phenomena in the decay process of radon in air.

## References

1. E. Ancochea, J.M. Fuster, E. Ibarrola, A. Cendrero, J. Coello, F. Hernán, J.M. Cantagrel, C. Jamond, J. Volcanol. Geotherm Res. **44**, 231 (1990)
2. G.J. Ably, J. Marti, J. Volcanol. Geotherm Res. **103**, 175 (2000)
3. J.C. Carracedo, E. Rodríguez, H. Guillou, M. Paterne, S. Scaillet, F. Pérez, R. Paris, U. Fra-Paleo, A. Hansen, GSA Bulletin **119**, 1027 (2007)
4. C. Martin-Luis, PhD Thesis, University of La Laguna, Tenerife, 1999
5. C. Martin-Luis, M.L. Quesada, A. Eff-Darwich, J. De la Nuez, J. Coello, A. Ahijado, R. Casillas, V. Soler. Environ. Geol. **43**, 72 (2002)
6. A. Eff-Darwich, C. Martin-Luis, M. Quesada, J. de la Nuez, J. Coello. Geophys. Res. Lett. **29**, 2069 (2002)
7. V. Soler, J.A. Castro-Almazán, R.T. Viñas, A. Eff-Darwich, S. Sanchez-Moral, C. Hillaire-Marcel, I. Farrujia, J. Coello, J. de la Nuez, M.C. Martin, M.L. Quesada, E. Santana, Pure Appl. Geophys. **161**, 1519 (2004)
8. G. Steinitz, M.C. Martin, N. Gazit-Yaari, M.L. Quesada, J. de la Nuez, R. Casillas, U. Malik, Z.B. Begin, Appl. Radiat. Isotopes **64**, 520 (2006)
9. R. Viñas, A. Eff-Darwich, V. Soler, M.C. Martin-Luis, M.L. Quesada, J. de la Nuez, Radiat. Meas. **42**, 101 (2007)
10. A. Eff-Darwich, R. Viñas, V. Soler, J. de la Nuez, M.L. Quesada, Radiat. Meas. **43**, 1429 (2008)
11. G. Steinitz, P. Kotlarsky, O. Piatibratova, Geophys. J. Internat. **193**, 1110 (2013)
12. G. Steinitz, O. Piatibratova, S.M. Barbosa, J. Geophys. Res. **112**, B10211 (2007)
13. G. Steinitz, O. Piatibratova, Geophys. J. Int. **180**, 651 (2010)
14. G. Steinitz, O. Piatibratova, Solid Earth **1**, 99 (2010)
15. G. Steinitz, O. Piatibratova, P. Kotlarsky, J. Environ. Rad. **102**, 749 (2011)
16. P.A. Sturrock, G. Steinitz, E. Fischbach, D. Javorsek, J.H. Jenkins, Astropart. Phys. **36**, 18 (2012)
17. G. Steinitz, O. Piatibratova, N. Charit-Yaari, Proc. R. Soc. A. **469**, 20130411 (2013)
18. I. Farrujia, J. Braojos, J. Fernandez, in *Proceedings of the VII Simposio de Hidrogeología de la Asociación Española de Hidrogeólogos* (Murcia, 2001), p. 661
19. N. Florea, O.G. Dului, J. Environ. Rad. **104**, 14 (2012)